

Fast and exact simulation of complex-valued stationary Gaussian processes through embedding circulant matrix

Jean-Francois Coeurjolly¹ and Emilio Porcu²

¹Laboratory Jean Kuntzmann, Grenoble Alpes University, France,

`Jean-Francois.Coeurjolly@upmf-grenoble.fr`

²Department of Mathematics, Technical University Federico Santa Maria, Chile,

`emilio.porcu@usm.cl`

March 3, 2022

Abstract

This paper is concerned with the study of the embedding circulant matrix method to simulate stationary complex-valued Gaussian sequences. The method is, in particular, shown to be well-suited to generate circularly-symmetric stationary Gaussian processes. We provide simple conditions on the complex covariance function ensuring the theoretical validity of the minimal embedding circulant matrix method. We show that these conditions are satisfied by many examples and illustrate the algorithm. In particular, we present a simulation study involving the circularly-symmetric fractional Brownian motion, a model introduced in this paper.

Keywords: Circularly-symmetric processes; Complex fractional Brownian motion; Positive definiteness.

1 Introduction

Complex-valued Gaussian processes have emerged in a wide variety of domains and applications, such as physics, engineering sciences, signal processing (see e.g. Curtis (1985); Dunmire *et al.* (2000); Amblard *et al.* (1996)), digital communication (Lee and Messerschmitt, 1994), climate modelling (Tobar and Turner, 2015). The present paper focusses on fast and exact simulation of a discretized sample path from a stationary complex-valued Gaussian sequence. By fast, we mean that the method can be applied for very large sample sizes, and by exact, we mean that the output vector has the expected covariance matrix.

The simulation of stationary Gaussian sequences is an important problem which has generated an important literature. Amongst available methods, the embedding circulant matrix method is probably the most popular as a very efficient alternative to methods based on the Cholesky decomposition. Introduced by Davies and Harte (1987), the method has been popularized by Wood and Chan (1994). The main idea is to embed the covariance matrix, say $\mathbf{\Gamma}$, of the stationary sequence to be simulated, into a circulant matrix \mathbf{C} . Unlike the diagonalization of $\mathbf{\Gamma}$, which can be computationally intensive for large sample sizes, the diagonalization of \mathbf{C} can be efficiently performed using the Fast Fourier Transform since, as a circulant matrix, \mathbf{C} is diagonalizable in the Fourier basis. For n being the sample size, the computational cost of the embedding circulant matrix method is $\mathcal{O}(n \log n)$, which considerably mitigates the computational burden of Cholesky decomposition methods, being of the order $\mathcal{O}(n^2)$ for Teoplitz matrices.

A non trivial requirement of circulant embedding method is that the matrix \mathbf{C} must be non-negative. This problem has also been the focus of several papers, and we especially refer to Dietrich and Newsam (1997) and Craigmile (2003) for simple and verifiable conditions on the covariance function, ensuring the non-negativeness of \mathbf{C} . It is noticeable that the combination of these two works covers elaborate models, such as the fractional Brownian motion (see e.g. Coeurjolly (2000) and the FARIMA model (see e.g. Brockwell and Davis (1987)).

Since the 90's, the embedding circulant matrix method has been extended in

many directions. Chan and Wood (1999) extended their algorithm to generate stationary univariate or multivariate random fields, as well as multivariate time series. This technical paper has recently been revisited by Helgason *et al.* (2011) for multivariate time series. In particular, the authors provided conditions ensuring the validity of the embedding circulant matrix method. In the context of random fields, the method has also known many developments by e.g. Stein (2002), Gneiting *et al.* (2012), Davies and Bryant (2013), Helgason *et al.* (2014) among others.

To generate a complex-valued stationary Gaussian sequence with given complex-valued covariance function, one can obviously simulate the corresponding real-valued bivariate stationary Gaussian process, and take the first (resp. second) component to define the real (resp. imaginary) part of the complex-valued stationary sequence to be simulated. This strategy, however, does not exploit the fact that any circulant Hermitian matrix can still be diagonalized using the Fourier basis. Percival (2006) indeed noticed this, and proposed an algorithm to generate a stationary complex-valued sequence with given complex-valued covariance matrix $\mathbf{\Gamma}$.

In order to characterize a complex-valued Gaussian process, covariance and pseudo covariance are both needed (see Section 2 for more details). This paper digs into the algorithms proposed by Wood and Chan (1994) and Percival (2006). Special emphasis is put on understanding the consequences on the control of the pseudo-covariance matrix. In addition, following the works by Dietrich and Newsam (1997) and Craigmile (2003), we provide conditions which ensure the validity of the minimal embedding circulant matrix method in the complex case.

The rest of the paper is organized as follows. Section 2 presents our main notation, provides a short background and details several examples. The simulation algorithms as well as an approximation, in the case where \mathbf{C} is negative, are presented in Section 3. Section 4 is focused on the theoretical validation of the embedding circulant matrix method for complex processes. We return to the examples in Section 5. We apply our theoretical conditions and illustrate the algorithms. In this section, we also use the simulation algorithm to compare several confidence intervals for the Hurst parameter of the circularly complex fractional Brownian motion, a model introduced in Section 2. Finally, proofs of our results are postponed to Appendix.

2 Background and notation

We denote $Z = \{Z(t)\}_{t \in S}$ a strictly stationary and complex-valued Gaussian process with index set S being either the real line, \mathbb{R} or the set of integers, \mathbb{Z} , or subsets of them. Since Z is complex-valued, it can be uniquely written as $Z(t) = Z_{\mathcal{R}}(t) + \mathbf{i}Z_{\mathcal{I}}(t)$, for $t \in S$, with \mathbf{i} being the complex number verifying $\mathbf{i}^2 = -1$. In particular, $Z_{\mathcal{R}}$ and $Z_{\mathcal{I}}$ are called real and imaginary parts, respectively, and the bivariate stochastic process $\{Z_{\mathcal{R}}(t), Z_{\mathcal{I}}(t)\}_{t \in S}$ is also stationary. The assumption of Gaussianity on Z implies that the finite dimensional distributions are uniquely determined through the second order properties of Z . In particular, we define the covariance function $\gamma : S \rightarrow \mathbb{C}$, through

$$\gamma(\tau) = \mathbb{E} \{Z(t + \tau)Z^*(t)\}, \quad t, \tau \in S,$$

where $*$ stands for the transpose conjugate operator. Covariance functions are positive definite: for any finite system of complex constants $(c_k)_{k=1, \dots, N} \subset \mathbb{C}$, and points t_1, \dots, t_N of S , we have $\sum_{j,k} c_j \gamma(t_j - t_k) c_k^* \geq 0$. We analogously define the cross covariances $\gamma_{\mathcal{R}, \mathcal{I}}$ and $\gamma_{\mathcal{I}, \mathcal{R}}$, as $\gamma_{\mathcal{R}, \mathcal{I}}(\tau) = \mathbb{E} \{Z_{\mathcal{R}}(t + \tau)Z_{\mathcal{I}}^*(t)\}$, for $t, \tau \in S$, and $\gamma_{\mathcal{I}, \mathcal{R}}(\tau) = \mathbb{E} \{Z_{\mathcal{I}}(t + \tau)Z_{\mathcal{R}}^*(t)\}$. A relevant remark is that $\gamma_{\mathcal{R}, \mathcal{I}}$ and $\gamma_{\mathcal{I}, \mathcal{R}}$ are not, in general, positive definite. Instead, the matrix-valued mapping

$$\begin{pmatrix} \gamma_{\mathcal{R}}(\tau) & \gamma_{\mathcal{R}, \mathcal{I}}(\tau) \\ \gamma_{\mathcal{I}, \mathcal{R}}(\tau) & \gamma_{\mathcal{I}}(\tau) \end{pmatrix}$$

with $\gamma_j \equiv \gamma_{jj}$, $j = \mathcal{R}, \mathcal{I}$, is positive definite according to previous definition, and it is precisely the covariance mapping associated to the stochastic process $\{Z_{\mathcal{R}}(t), Z_{\mathcal{I}}(t)\}_{t \in S}$. The following identity is true:

$$\gamma(\tau) = \gamma_{\mathcal{R}}(\tau) + \gamma_{\mathcal{I}}(\tau) + \mathbf{i} \{\gamma_{\mathcal{R}, \mathcal{I}}(\tau) - \gamma_{\mathcal{I}, \mathcal{R}}(\tau)\} = \gamma^*(-\tau), \quad \tau \in S,$$

where it is useful to note that, for $j, k = \mathcal{R}$ or \mathcal{I} , $\gamma_{jk}(\tau) = \gamma_{kj}(-\tau)$.

The aim of the present paper is to generate a discrete sample path of the process Z at times $j = 0, 1, \dots, n-1$, that is to generate a complex normal vector $\mathbf{Z} = \{Z(0), \dots, Z(n-1)\}^\top$ with length n , zero mean and with covariance matrix $\mathbf{\Gamma} =$

$E(\mathbf{Z}\mathbf{Z}^*)$ given by

$$\mathbf{\Gamma} = \begin{pmatrix} \gamma(0) & \gamma^*(1) & \dots & \gamma^*(n-2) & \gamma^*(n-1) \\ \gamma(1) & \gamma(0) & \gamma^*(1) & \vdots & \gamma^*(n-2) \\ \vdots & \ddots & \ddots & \ddots & \vdots \\ \gamma(n-2) & \gamma(n-3) & \dots & \gamma(0) & \gamma^*(1) \\ \gamma(n-1) & \gamma(n-2) & \dots & \gamma(1) & \gamma(0) \end{pmatrix}. \quad (2.1)$$

The covariance function γ does not determine uniquely the properties of a complex-valued Gaussian process. This can be achieved if, in addition to γ , the complementary autocovariance function (also called the relation or pseudo-covariance function) $h : S \rightarrow \mathbb{R}$, defined through $h(\tau) = E\{Z(t+\tau)Z(t)\}$, is given (see e.g. Lee and Messerschmitt (1994, Chapter 8)), the class of circularly-symmetric processes being an exception. A complex-valued process is said to be circularly-symmetric if $h(\tau) = 0$ for any $\tau \in S$, in which case a stationary complex-valued Gaussian process is uniquely determined by its covariance function. Elementary calculations show that for circularly-symmetric stationary processes

$$\gamma_{\mathcal{R}}(\tau) = \gamma_{\mathcal{I}}(\tau) \quad \text{and} \quad \gamma_{\mathcal{R}\mathcal{I}}(\tau) = -\gamma_{\mathcal{I}\mathcal{R}}(\tau) = -\gamma_{\mathcal{R}\mathcal{I}}(-\tau), \quad \tau \in S.$$

For a given class of pseudo-covariances, we can define the matrix $\mathbf{H} = E(\mathbf{Z}\mathbf{Z}^\top)$. In this paper, we propose an algorithm for generating a complex-valued Gaussian vector with prescribed covariance matrix $\mathbf{\Gamma}$. We do not focus on the matrix \mathbf{H} , which will be controlled a posteriori, the class of circularly-symmetric processes being again a notable exception. For example, The Cholesky decomposition method decomposes $\mathbf{\Gamma}$ as $\mathbf{L}\mathbf{L}^*$ where \mathbf{L} is a lower triangular matrix and sets $\mathbf{Z} = \mathbf{L}\mathbf{N}_n$ where \mathbf{N}_n is a centered complex Gaussian vector with identity covariance matrix. In particular, we can check that if \mathbf{N}_n is real, $E(\mathbf{N}_n\mathbf{N}_n^*) = E(\mathbf{N}_n\mathbf{N}_n^\top) = \mathbf{I}_n$ and the covariance and relation matrices are respectively equal to $\mathbf{\Gamma}$ and $\mathbf{H} = \mathbf{L}\mathbf{L}^\top$, that is $\mathbf{Z} \sim CN(0, \mathbf{\Gamma}, \mathbf{H})$, with CN meaning complex normal. If \mathbf{N}_n is a circular centered complex normal random vector with identity covariance matrix, then $\mathbf{Z} \sim CN(0, \mathbf{\Gamma}, \mathbf{0})$.

To generate a complex normal vector \mathbf{Z} with covariance matrix $\mathbf{\Gamma}$ and pseudo-covariance matrix \mathbf{H} , from a complex stationary process Z , one can simulate the bivariate Gaussian vector $(\mathbf{Z}_{\mathcal{R}}, \mathbf{Z}_{\mathcal{I}})$ from the bivariate stationary process $(Z_{\mathcal{R}}, Z_{\mathcal{I}})$,

and set $\mathbf{Z} = \mathbf{Z}_{\mathcal{R}} + \mathbf{i}\mathbf{Z}_{\mathcal{I}}$. The simulation of multivariate Gaussian time series is considered by Chan and Wood (1999) and has been nicely revisited by Helgason *et al.* (2011). We did not consider this direction in this paper as we aimed to exploit the complex characteristic of the process Z . Doing this, our algorithm, except for circularly-symmetric processes, does not control beforehand the pseudo-covariance, but its computational cost is clearly smaller than the one required to generate a bivariate Gaussian time series. Moreover, the algorithms proposed by Chan and Wood (1999) and Helgason *et al.* (2011) obviously require the covariance functions $\gamma_{\mathcal{R}}$ and $\gamma_{\mathcal{I}}$, as well as the cross-covariance functions $\gamma_{\mathcal{RI}}$ and $\gamma_{\mathcal{IR}}$, to be given. Instead, the method described in the next section will only assume the complex covariance function γ to be given. Such a construction seems to be more natural especially for circularly-symmetric Gaussian processes.

Example 2.1 (Modulated stationary process). Let $r : S \rightarrow \mathbb{R}$ be the covariance function of a real-valued, Gaussian, and stationary stochastic process $\{Y(t)\}_{t \in S}$. Let Z be the complex-valued Gaussian process defined as $Z(t) = e^{2i\pi t}Y(t)$, $t \in S$ and $\phi \in \mathbb{R}$. Then, straightforward calculations show that

$$\gamma(\tau) = e^{2i\pi\phi\tau}r(\tau), \quad \tau \in S \quad (2.2)$$

is the covariance function of Z , which is called a modulated Gaussian process. Similar constructions can then be implemented using the fact that covariance functions are a convex cone being closed under the topology of finite measures. For instance, for a collection of p uncorrelated real-valued Gaussian processes Y_k with covariance r_k , the complex-valued Gaussian process, defined through $Z(t) = \sum_k^p e^{2i\pi\phi_k t}Y_k(t)$, $t \in S$, for $\phi_k \in \mathbb{R}$ for all $k = 1, \dots, p$, has covariance function

$$\gamma(\tau) = \sum_{j=1}^p e^{2i\pi\phi_j\tau}r_j(\tau), \quad \tau \in S \quad (2.3)$$

Remarkably, for such a construction, the range of dependence, defined as the lag beyond which becomes negligible, is the maximum of the ranges related to each of the covariances r_k . Let us list a few examples from this construction:

- Exponential modulated process: let $p = 1$, under the exponential model $r(\tau) = \sigma^2 e^{-\alpha\tau}$, where σ^2 is the variance and $0 < \alpha$ a scaling parameter, the related

construction leads to

$$\gamma(\tau) = \sigma^2 e^{-\alpha\tau + 2i\pi\phi\tau}, \quad \tau \in S. \quad (2.4)$$

- Complex autoregressive process of order 1: this process is defined by the equation

$$Z(t) - aZ(t-1) = \varepsilon(t), \quad t \in \mathbb{Z}$$

where $a \in \mathbb{C}$ such that $|a| < 1$ and $\{\varepsilon(t)\}_{t \in \mathbb{Z}}$ is a complex normal white noise with variance σ^2 . Then, Z is a stationary process and its covariance function is given for any τ by $\gamma(\tau) = a^{|\tau|} \sigma^2 (1 - |a|^2)^{-1}$. If the white noise is circularly-symmetric then so is Z . Finally, letting $a = \rho e^{2i\pi\phi}$, we note that $\gamma(\tau) = e^{2i\pi\phi\tau} \rho^{|\tau|} \sigma^2 (1 - |\rho|) = e^{2i\pi\phi\tau} r(\tau)$ where r is the covariance function of a stationary real-valued AR(1) process.

- Percival (2006) considered for example the sum of two modulated covariance functions of FARIMA processes

$$\gamma(\tau) = \sum_{k=1}^2 e^{2i\pi\phi_k\tau} r(\tau; d_k), \quad \tau \in S$$

where $r(\cdot; d)$ is the autocovariance function of a FARIMA process with fractional difference parameter $d \in [-1/2, 1/2]$, and with innovations variance σ_ε^2 given for $\tau \in \mathbb{N}$, by, see e.g. Brockwell and Davis (1987),

$$r(\tau; d) = \sigma_\varepsilon^2 \frac{(-1)^\tau \Gamma(1 - 2d)}{\Gamma(1 - d + \tau) \Gamma(1 - d - \tau)}. \quad (2.5)$$

On the basis of this construction, when $p = 1$, a realization of \mathbf{Z} can be simply obtained as follows: generate two independent realizations \mathbf{Y}_1 and \mathbf{Y}_2 of Y at times $0, 1, \dots, n-1$ using, for instance, the embedding circulant matrix method for real-valued stationary Gaussian processes (Wood and Chan, 1994). Then, set $(\mathbf{Z}_j)_\ell = e^{i\phi\ell} (\mathbf{Y}_j)_\ell$, $j = 1, 2$. Finally, obtain the realization \mathbf{Z} through the identity $\mathbf{Z} = \mathbf{Z}_1 + i\mathbf{Z}_2$. The latter has the desired covariance matrix and is ensured to be circular. When $p > 1$ this strategy can still be extended but is more computationally intensive and less natural than directly simulate a circular complex normal vector with the right covariance function.

Example 2.2 (Complex fractional Brownian motion). We define the complex fractional Brownian motion as the self-similar Gaussian process \tilde{Z} , equal to zero at zero, with stationary increments. The self-similarity property is understood as

$$\tilde{Z}(\lambda t) \stackrel{fidi}{=} \lambda^H \tilde{Z}(t) \iff \tilde{Z}_j(\lambda t) \stackrel{fidi}{=} \lambda^H \tilde{Z}_j(t), \quad j = \mathcal{R}, \mathcal{I} \quad (2.6)$$

where $t \in \mathbb{R}$, $H \in (0, 1)$ is called the Hurst exponent, λ is any non-negative real number, the sign $\stackrel{fidi}{=}$ means equality in distribution for all finite-dimensional margins and $\tilde{Z}_{\mathcal{R}}(t)$ (resp. $\tilde{Z}_{\mathcal{I}}(t)$) is the real part (resp. imaginary part) of $\tilde{Z}(t)$. The self-similarity property (2.6) is equivalent to $\{\tilde{Z}_{\mathcal{R}}(\lambda t), \tilde{Z}_{\mathcal{I}}(\lambda t)\} = \lambda^H \{\tilde{Z}_{\mathcal{R}}(t), \tilde{Z}_{\mathcal{I}}(t)\}$, a model called the multivariate fractional Brownian motion, a particular case of operator fractional Brownian motion (Didier and Pipiras, 2011), and studied by Amblard *et al.* (2013); Coeurjolly *et al.* (2013). As a direct consequence of these works, the increments process, denoted by $Z = \{Z(t)\}_{t \in \mathbb{R}}$, defined by $Z(t) = \tilde{Z}(t+1) - \tilde{Z}(t)$ and referred to as the complex fractional Gaussian noise has covariance function γ parameterized, when $H \neq 1/2$, as

$$\gamma(\tau) = \frac{1}{2} \{ \sigma_{\mathcal{R}}^2 + \sigma_{\mathcal{I}}^2 - 2\mathbf{i} \eta \sigma_{\mathcal{R}} \sigma_{\mathcal{I}} \text{sign}(\tau) \} (|\tau - 1|^{2H} - 2|\tau|^{2H} + |\tau + 1|^{2H}) \quad (2.7)$$

where $\sigma_{\mathcal{R}} = \mathbb{E}\{Z_{\mathcal{R}}(1)\}^{1/2}$ and $\sigma_{\mathcal{I}} = \mathbb{E}\{Z_{\mathcal{I}}(1)\}^{1/2}$ are non-negative real numbers and $\eta \in \mathbb{R}$. When $H = 1/2$ another parameterization occurs and for the ease of the presentation, we avoid this case. Amblard *et al.* (2013, Proposition 9) states that the covariance function (2.7) is a valid covariance function if and only if $\eta^2 \leq \tan(\pi H)^2$.

When the process is time-reversible, i.e. $\tilde{Z}(t) \stackrel{d}{=} \tilde{Z}(-t)$ for any $t \in \mathbb{R}$ then, as outlined by Amblard *et al.* (2013), the parameter η must be equal to zero, which makes the covariance function γ real. This is not of special interest for this paper. Finally, when $\sigma_{\mathcal{R}} = \sigma_{\mathcal{I}} = \sigma$, the covariance function reduces to

$$\gamma(\tau) = \sigma^2 \{1 - \mathbf{i} \eta \text{sign}(\tau)\} (|\tau - 1|^{2H} - 2|\tau|^{2H} + |\tau + 1|^{2H}) \quad (2.8)$$

and it can be checked that the corresponding stochastic process Z is circularly-symmetric.

3 Simulation through circulant matrix method

This section deals with circulant embedding method for complex-valued covariance functions. The procedure is an extension of the standard method proposed by Wood and Chan (1994) for real covariance functions. It is also slightly different from the extension proposed by Percival (2006) to handle complex covariance functions. Then, we discuss the main question of this method which is the non-negativeness of the circulant matrix in which $\mathbf{\Gamma}$ is embedded.

3.1 Simulation of a complex normal vector with covariance matrix $\mathbf{\Gamma}$

In order to achieve a realization from the Gaussian process Z , under the covariance function γ , at times $0, 1, \dots, n-1$, we need to obtain a realization from \mathbf{Z} being complex normal, with covariance matrix $\mathbf{\Gamma}$ given by (2.1).

Let $m \geq n-1$, $\tilde{m} = 2m+1$ and let \mathbf{C} be the $\tilde{m} \times \tilde{m}$ circulant matrix defined by its first row $\{c_j, j = 0, \dots, 2m\}$, where

$$c_j = \begin{cases} \gamma(0) & \text{if } j = 0 \\ \gamma^*(j) & \text{if } j = 1, \dots, m \\ \gamma(2m+1-j) & \text{if } j = m+1, \dots, 2m. \end{cases} \quad (3.1)$$

By construction, the top left corner of \mathbf{C} corresponds to the covariance matrix $\mathbf{\Gamma}$. Standard results for symmetric circulant matrices, see Brockwell and Davis (1987), show that the Hermitian matrix \mathbf{C} can be decomposed as $\mathbf{C} = \mathbf{Q}\mathbf{\Lambda}\mathbf{Q}^*$, where $\mathbf{\Lambda} = \text{diag}\{\lambda_0, \dots, \lambda_{\tilde{m}-1}\}$ is the diagonal matrix of real eigenvalues of \mathbf{C} , \mathbf{Q} is the matrix with entries

$$(\mathbf{Q})_{jk} = \tilde{m}^{-1/2} e^{-\frac{2i\pi jk}{\tilde{m}}}, \quad j, k = 0, \dots, \tilde{m}-1. \quad (3.2)$$

If \mathbf{C} is non-negative, that is if $\lambda_k \geq 0$ for $k = 0, \dots, \tilde{m}-1$, the simulation method consists simply in picking the first n components of the vector $\mathbf{Q}\mathbf{\Lambda}^{1/2}\mathbf{Q}^*\mathbf{N}_{\tilde{m}}$ where $\mathbf{N}_{\tilde{m}}$ is a complex normal vector with mean 0 and identity covariance matrix. The main advantage being the fast computation of the eigenvalues, additionally with minimal storage when using Fast Fourier Transform (FFT).

The procedure proposed in this paper is similar to the algorithm proposed by Wood and Chan (1994), who worked in the real-valued case, and by Percival (2006) in the complex case. In particular, our first algorithm extends Wood and Chan (1994) and considers $\mathbf{N}_{\tilde{m}}$ as a real vector, that is a vector of \tilde{m} independent standard Gaussian random variables. The second algorithm, presented in Section 3.2 considers $\mathbf{N}_{\tilde{m}}$ as a circular complex normal vector with identity covariance matrix.

ALGORITHM 1.

Step 0. Let $m \geq n - 1$, be an odd number (preferably a highly composite number). Embed the matrix $\mathbf{\Gamma}$ into the circulant matrix \mathbf{C} given by (3.1).

Step 1. Determination of the eigenvalues $\lambda_0, \dots, \lambda_{\tilde{m}-1}$. The calculation of $\mathbf{\Lambda} = \mathbf{Q}^* \mathbf{C} \mathbf{Q}$ leads to

$$\lambda_k = \sum_{j=0}^{\tilde{m}-1} c_j e^{-\frac{2i\pi jk}{\tilde{m}}}, \quad k = 0, \dots, \tilde{m} - 1. \quad (3.3)$$

Check that all eigenvalues are non-negative (Section 4 provides some conditions on γ which ensure this fact). If some of them are negative, increase m and go back to Step 0 or set the negative eigenvalues to 0. With the latter option, discussed in more details in Section 3.3, the simulation will be only approximate.

Step 2. Simulation of $\mathbf{W} = \{W_0, \dots, W_{\tilde{m}-1}\}^\top = \tilde{m}^{-1/2} \mathbf{\Lambda}^{1/2} \mathbf{Q}^* \mathbf{N}_{\tilde{m}}$. This is achieved using the following result.

Proposition 3.1. *For $k = 0, \dots, \tilde{m} - 1$*

$$(\mathbf{W})_k = W_k = \sqrt{\frac{\lambda_k}{2\tilde{m}}} \times \begin{cases} S_k + iT_k & \text{for } k = 0, \dots, m \\ S_{\tilde{m}-k} - iT_{\tilde{m}-k} & \text{for } k = m + 1, \dots, \tilde{m} - 1, \end{cases}$$

in distribution, where for $k = 0, \dots, m$, S_k and T_k are real-valued Gaussian random variables with mean 0 and variance 1, and $S_0, \dots, S_m, T_0, \dots, T_m$ are mutually independent.

Step 3. Reconstruction of \mathbf{Z} . This step results in calculating $\mathbf{Q} \mathbf{\Lambda}^{1/2} \mathbf{Q}^* \mathbf{N}_{\tilde{m}} = \tilde{m}^{1/2} \mathbf{Q} \mathbf{W}$ and keep the first n components, which corresponds to the calculation of

$$(\mathbf{Z})_k = \sum_{j=0}^{\tilde{m}-1} W_j e^{-\frac{2i\pi jk}{\tilde{m}}}, \quad k = 0, \dots, n - 1. \quad (3.4)$$

Step 2 requires the simulation $2m+2$ independent realizations of standard Gaussian random variables. This is computationally less expensive than the similar step of the algorithm proposed by Percival (2006), which, with the notation of the present paper, requires $4m$ realizations of Gaussian variables. Since $\tilde{m} = 2m + 1$ is an odd number, the proof of Step 2 is also slightly different from Wood and Chan (1994, Proposition 3.3). Steps 1 and 3 can be handled very quickly using the direct FFT.

Some comments are in order. In the real-valued case, $\mathbf{\Gamma}$ is real and symmetric by construction. In particular, we have $\gamma(m) = \gamma^*(m)$, so that the dimension of \mathbf{C} can be reduced to $2m \times 2m$, where m is an integer being larger than $2(n-1)$, and $2m$ can be set to a power of two. In the complex-valued case, \mathbf{C} has dimension $(2m+1) \times (2m+1)$, with $(2m+1)$ being necessarily an odd number.

Percival (2006) used a specific modulation of the initial process Z to force $\gamma(m)$ to be real, that is instead of generating \mathbf{Z} with covariance matrix $\mathbf{\Gamma}$, the idea is to generate $\check{\mathbf{Z}} = \{e^{i\nu k}(\mathbf{Z})_k\}_{k=1,\dots,n}$ where ν is chosen such that $e^{i\nu m}\gamma^*(m)$ is a real number. This modulation enables to recover a circulant matrix \mathbf{C} with dimension $2m \times 2m$, $2m$ can still be set to a power of two, which allows the use of 'powers of two' FFT algorithm for diagonalizing \mathbf{C} . Forcing $\gamma(m)$ to be real has however some minor drawbacks: first, if we increase the value of m , the modulation changes and the first row of \mathbf{C} is completely modified. Second, the introduction of the modulation modifies the covariance function γ . The resulting covariance function is less easy to handle from a theoretical point of view, in particular when we want to provide conditions on γ ensuring \mathbf{C} to be non-negative.

Defining \mathbf{C} by (3.1) imposes the number of rows to be an odd number. However, this is not of great importance because FFT algorithm (like the one implemented in the R function `fft`) is very efficient when $2m+1$ is highly composite, that is has many factors, see Brockwell and Davis (1987) or Numerical Algorithms Group (1993). We explore this in Table 1. Remind that n is the length of the desired sample path of Z . Using a specific modulation of Z , Percival (2006) suggested to use a minimal embedding which corresponds to a circulant matrix whose first row length, denoted by \tilde{m}_{mod} , is the first power of 2 larger $2(n-1)$. When \mathbf{C} is defined by (3.1), we let \tilde{m}

be the first power of 3, 5, 7, 11 or a combination of these powers larger than $2n - 1$. Table 1 reports average time in milliseconds of FFT algorithm applied to vector of length equal to \tilde{m}_{mod} or \tilde{m} for different values of n . For the values of n considered in Table 1, we can always find a highly composite integer number $\tilde{m} < \tilde{m}_{\text{mod}}$. As a consequence of this, we observe a time reduction when a FFT is applied whereby we conclude that there is no reason to focus on embedding into a circulant matrix with first row as a power of two. Therefore, we did not consider the modulation suggested by Percival (2006).

	n=1000	5000	10000	50000	100000	500000	1000000
$\tilde{m}_{\text{mod}} = 2^p$	0	1	2	13	25	210	470
$\tilde{m} = 3^p$	0	1	3	10	82	331	1258
5^p	0	1	4	47	47	369	2553
7^p	0	1	7	8	136	1319	1343
11^p	1	1	10	10	296	282	5106
$3^{p_1} 5^{p_2}$	0	0	2	6	15	198	410
$3^{p_1} 5^{p_2} 7^{p_3}$	1	1	2	6	12	173	439
$3^{p_1} 5^{p_2} 7^{p_3} 11^{p_4}$	0	1	1	6	12	169	383

Table 1: Average time (in ms) of FFT applied to vectors (obtained as realizations of standard Gaussian random variables) of length \tilde{m}_{mod} or \tilde{m} . Ten replications are considered. We restrict attention on the cases $p_3 \geq 1$ and $p_1 \wedge p_2 > 0$ for the second to last row and on the cases $p_4 \geq 1$ and $p_1 \wedge p_2 \wedge p_3 > 0$ for the last row. Experiments are performed on a 1.7 GHz Intel Core i7 processor.

ALGORITHM 1 does not control the relation matrix \mathbf{H} but we can have an idea of its form. This is given by the following result.

Proposition 3.2. *Let $\mathbf{Z}_{\tilde{m}}$ be the output vector of ALGORITHM 1, then the relation matrix \mathbf{H} of $\mathbf{Z} = (\mathbf{Z}_{\tilde{m}})_{0:(n-1)}$ corresponds to the top left corner of $\mathbf{H}_{\tilde{m}} = \mathbf{E} \mathbf{Z}_{\tilde{m}} \mathbf{Z}_{\tilde{m}}^\top = \mathbf{Q}^* \mathbf{V} \mathbf{Q}$ where $\mathbf{V} = \text{diag}(v_k, k = 0, \dots, \tilde{m} - 1)$ is the diagonal matrix with elements given by $v_0 = 0$ and $v_k = \sqrt{\lambda_k \lambda_{\tilde{m}-k}}$ for $k \geq 1$, where $\lambda_k, k = 0, \dots, \tilde{m} - 1$ are the eigenvalues of \mathbf{C} given by (3.3). Thus, $\mathbf{Q}^* \mathbf{V} \mathbf{Q}$ is necessarily a circulant matrix and*

\mathbf{H} is necessarily a Toeplitz Hermitian matrix with first row given by

$$\mathbf{H}_{0k} = \sum_{j=1}^{\tilde{m}-1} \sqrt{\lambda_j \lambda_{\tilde{m}-j}} e^{-\frac{2i\pi jk}{\tilde{m}}}.$$

3.2 Simulation of a circular complex normal with covariance matrix $\mathbf{\Gamma}$

This section focusses on the circularly symmetric case, for which $\mathbf{H} = \mathbf{0}$. A realization \mathbf{Z} from such a process can be obtained as follows: let \mathbf{Z}_1 and \mathbf{Z}_2 be two output vectors from ALGORITHM 1. Then, set $\mathbf{Z} = (\mathbf{Z}_1 + i\mathbf{Z}_2)/\sqrt{2}$. This in turn results in a modification of ALGORITHM 1: in Step 2, $\mathbf{N}_{\tilde{m}}$ is replaced by a circular complex normal random vector, i.e. the vector $(\mathbf{N}_{1,\tilde{m}} + i\mathbf{N}_{2,\tilde{m}})/\sqrt{2}$ where $\mathbf{N}_{1,\tilde{m}}$ and $\mathbf{N}_{2,\tilde{m}}$ are two real-valued, mutually independent, random vectors of independent standard Gaussian random variables.

ALGORITHM 2.

Steps 0 and 1. Similar to Steps 0 and 1 of ALGORITHM 1.

Step 2. Simulation of $\mathbf{W} = \{W_0, \dots, W_{\tilde{m}-1}\}^\top = \tilde{m}^{-1/2} \mathbf{\Lambda}^{1/2} \mathbf{Q}^* (\mathbf{N}_{1,\tilde{m}} + i\mathbf{N}_{2,\tilde{m}})/\sqrt{2}$. This is achieved using the following result.

Proposition 3.3. *For $k = 0, \dots, \tilde{m} - 1$,*

$$W_k = \sqrt{\frac{\lambda_k}{2\tilde{m}}} (S_k + iT_k)$$

in distribution, where for $k = 0, \dots, m$, S_k and T_k are Gaussian random variables with mean 0 and variance 1, and $S_0, \dots, S_m, T_0, \dots, T_m$ are mutually independent.

Step 3. Similar to Step 3 of ALGORITHM 1.

It is worth noticing that Step 2 of ALGORITHM 2 now requires the simulation of $4m + 2$ realizations of standard Gaussian distributions and is very similar to the corresponding step of the algorithm proposed by Percival (2006).

We think the distinctions we make between the two algorithms we propose, make more clear the understanding of the consequences of each algorithm on the relation matrix \mathbf{H} .

3.3 Approximation and error control

In this section, we focus on circularly-symmetric processes and propose a modification of ALGORITHM 2 when \mathbf{C} is negative. When, it is practically unfeasible to increase the value of m and reperform Steps 0 and 1, we follow Wood and Chan (1994) and suggest to truncate the eigenvalues to 0. The simulation becomes only approximate.

This section details the procedure and provides a control of the approximation error. We decompose \mathbf{C} as follows

$$\mathbf{C} = \mathbf{Q}\mathbf{\Lambda}\mathbf{Q}^* = \mathbf{Q}(\mathbf{\Lambda}_+ - \mathbf{\Lambda}_-)\mathbf{Q}^* = \mathbf{C}_+ - \mathbf{C}_-$$

where $\mathbf{\Lambda}_\pm = \text{diag}\{\max(0, \pm\lambda_k), k = 0, \dots, \tilde{m}-1\}$. We suggest to replace \mathbf{C} in Step 1 by $\varphi^2\mathbf{C}_+$ with $\varphi = \text{tr}(\mathbf{\Lambda})/\text{tr}(\mathbf{\Lambda}_+)$. Let \mathbf{Z}^{app} be the output vector of ALGORITHM 2, which is a circular centered complex normal vector with covariance matrix $\mathbf{\Sigma}^{\text{app}}$ equal to the top left corner of $(\varphi^2\mathbf{C}_+)$. It is worth noticing that this choice for φ leads to $(\varphi^2\mathbf{C}_+)_{jj} = (\mathbf{\Sigma})_{jj}$, for $j = 0, \dots, n-1$. Let \mathbf{Z} be a complex normal vector independent of \mathbf{Z}^{app} , with zero mean and covariance matrix $\mathbf{\Sigma}$. We define $\mathbf{\Delta} = \mathbf{Z} - \mathbf{Z}^{\text{app}}$ as the random error of approximation. Clearly, $\mathbf{\Delta}$ is a circular centered complex normal vector with covariance matrix $\mathbf{\Sigma} - \mathbf{\Sigma}^{\text{app}}$. Using multivariate normal probabilities on rectangles proposed by Dunn (1958, 1959) (see also Tong (1982, chapter 2)), we obtain the following approximation.

Proposition 3.4. *Let $s_j^2 = \text{Var } \Delta_j$, $s_{j,\mathcal{R}}^2 = \text{Var } \text{Re}(\Delta_j)$ and $s_{j,\mathcal{I}}^2 = \text{Var } \text{Im}(\Delta_j)$, for $j = 0, \dots, n-1$. Then, for each $x > 0$*

$$\mathbb{P} \left(\max_{j=0, \dots, n-1} \sigma_j^{-1} |\Delta_j| > x \right) \leq 1 - \prod_{j=0}^{n-1} \prod_{k \in \mathcal{T}} \left\{ 2\Phi \left(\frac{x\sigma_j}{\sigma_{j,\mathcal{M}}\sqrt{2}} \right) - 1 \right\}, \quad (3.5)$$

for $\mathcal{T} = \{\mathcal{R}, \mathcal{I}\}$.

For different values of x , (3.5) can be used to control the largest normalized error.

4 Non-negativeness of \mathbf{C}

The condition ensuring the circulant matrix \mathbf{C} to be non-negative is now discussed. Dietrich and Newsam (1997) and Craigmile (2003) dealt with the real-valued case,

and combination of their results covers many interesting classes of covariance functions. We now show how to extend these results to the complex-valued case.

Let us first express the eigenvalues λ_k in terms of the covariance function γ . By (3.1) and (3.3), we have for any $k = 0, \dots, \tilde{m} - 1$

$$\begin{aligned}\lambda_k &= \gamma(0) + \sum_{j=1}^m \gamma^*(j) e^{-\frac{2i\pi jk}{\tilde{m}}} + \sum_{j=m+1}^{2m} \gamma(\tilde{m} - j) e^{-\frac{2i\pi jk}{\tilde{m}}} \\ &= \gamma(0) + \sum_{j=1}^m \left\{ \gamma^*(j) e^{-\frac{2i\pi jk}{\tilde{m}}} + \gamma(j) e^{\frac{2i\pi jk}{\tilde{m}}} \right\} \\ &= \gamma(0) + 2 \sum_{j=1}^m \left\{ \mathcal{R}(j) \cos\left(\frac{2\pi jk}{\tilde{m}}\right) - \mathcal{I}(j) \sin\left(\frac{2\pi jk}{\tilde{m}}\right) \right\},\end{aligned}\quad (4.1)$$

where \mathcal{R} and \mathcal{I} correspond to the real and imaginary parts of the complex covariance function γ , that is $\mathcal{R}(j) = \gamma_{\mathcal{R}}(j) + \gamma_{\mathcal{I}}(j)$ and $\mathcal{I}(j) = \gamma_{\mathcal{R}\mathcal{I}}(j) - \gamma_{\mathcal{I}\mathcal{R}}(j)$.

The first result extends the main result of Craigmile (2003).

Proposition 4.1. *For any integer $m \geq n - 1$, let λ_k , $k = 0, \dots, \tilde{m} - 1$ as defined through Equation (4.1). Then, either of the following conditions are sufficient for λ_k to be non-negative for all k .*

(i) *For $j \in \mathbb{Z} \setminus \{0\}$, $\mathcal{R}(j)$ is negative and $s = \text{sign}\{j\mathcal{I}(j)\}$ is constant. Additionally, for any $j \in \mathbb{Z}$, the matrix*

$$\mathbf{M}(j) = \begin{pmatrix} \gamma_{\mathcal{R}}(j) & \text{sign}(j)\gamma_{\mathcal{R}\mathcal{I}}(j) \\ -\text{sign}(j)\gamma_{\mathcal{I}\mathcal{R}}(j) & \gamma_{\mathcal{I}}(j) \end{pmatrix} \quad (4.2)$$

is the covariance matrix of a bivariate stationary process on \mathbb{Z} which admits a well-defined spectral density matrix \mathbf{S} .

(ii) *For a circularly-symmetric stationary process Z such that $\gamma_{\mathcal{R}\mathcal{I}}(j) = \eta \text{sign}(j) \gamma_{\mathcal{R}}(j)$ for $j \neq 0$ for some parameter $\eta \in [-1, 1]$, and such that $\gamma_{\mathcal{R}}(j)$ is negative for $j \geq 1$.*

(iii) *The covariance function γ is defined according to Equation (2.2) and $r \geq 0$ on \mathbb{Z}_+ .*

The next result extends Dietrich and Newsam (1997, Theorem 2). For a sequence $(f_k)_{k \geq 0}$ of real numbers, we denote the first and second order finite differences by $\Delta f_k = f_k - f_{k+1}$ and $\Delta^2 f_k = \Delta f_k - \Delta f_{k+1}$. The sequence (f_0, \dots, f_k, \dots) is said to be decreasing and convex respectively, if $\Delta f_k \geq 0$ and $\Delta^2 f_k \geq 0$ for $k \geq 0$.

Proposition 4.2. *Let the functions \tilde{D} , K and \tilde{K} be, respectively, the conjugate Dirichlet, the Féjer and conjugate Féjer kernels, as being defined in Lemma A.1 (Appendix). For any $k = 0, \dots, \tilde{m} - 1$, let λ_k as being defined through Equation (4.1). Then, it is true that*

$$\begin{aligned} \lambda_k = & -\mathcal{I}(m)\tilde{D}_m\left(\frac{k}{\tilde{m}}\right) + (-\Delta\mathcal{I})(m-1)\tilde{K}_{m-1}\left(\frac{k}{\tilde{m}}\right) + \sum_{j=1}^{m-2}(-\Delta^2\mathcal{I})(j)\tilde{K}_j\left(\frac{k}{\tilde{m}}\right) \\ & + \Delta\mathcal{R}(m-1)K_{m-1}\left(\frac{k}{\tilde{m}}\right) + \sum_{j=0}^{m-2}(\Delta^2\mathcal{R})(j)K_j\left(\frac{k}{\tilde{m}}\right). \end{aligned} \quad (4.3)$$

Also, for any integer $m \geq n - 1$, the following conditions are sufficient for λ_k to be non-negative:

(i) The two sequences $\{\mathcal{R}(0), \dots, \mathcal{R}(m)\}$ and $\{-\mathcal{I}(1), \dots, -\mathcal{I}(m)\}$ are both decreasing and convex, $-\mathcal{I}(m) \geq 0$ and

$$\Delta^2\mathcal{R}(0) + S_m \geq -\mathcal{I}(m) \quad (4.4)$$

where

$$S_m = \inf_{k=0, \dots, \tilde{m}-1} \sum_{j=1}^{m-2} \left\{ \Delta^2\mathcal{R}(j)K_j\left(\frac{k}{\tilde{m}}\right) - \Delta^2\mathcal{I}(j)\tilde{K}_j\left(\frac{k}{\tilde{m}}\right) \right\}.$$

(ii) For Z a circularly-symmetric stationary process such that $\gamma_{\mathcal{R}\mathcal{I}}(j) = -\eta \text{sign}(j)\gamma_{\mathcal{R}}(j)$ for $j \neq 0$ and some parameter $\eta > 0$, the sequence $\{\gamma_{\mathcal{R}}(0), \dots, \gamma_{\mathcal{R}}(m)\}$ is decreasing and convex, with $\gamma_{\mathcal{R}}(m) \geq 0$ and

$$\Delta^2\gamma_{\mathcal{R}}(0) + S_m(\eta) \geq \eta\gamma_{\mathcal{R}}(m) \quad (4.5)$$

where

$$S_m(\eta) = \inf_{k=0, \dots, \tilde{m}-1} \sum_{j=1}^{m-2} \Delta^2\gamma_{\mathcal{R}}(j) \left\{ K_j\left(\frac{k}{\tilde{m}}\right) + \eta\tilde{K}_j\left(\frac{k}{\tilde{m}}\right) \right\}.$$

Remark 4.3. By Lemma A.1, the Féjer kernel is always non-negative. The conjugate Féjer kernel is also non-negative for any k such that $k/\tilde{m} < 1/2$. Therefore, the infimum involved in conditions (4.4) and (4.5) can be taken over the set $\{m+1, \dots, \tilde{m}-1\}$. This term S_m could look annoying as it seems to depend strongly on m . We investigate this in Section 5.1 on a specific example.

Remark 4.4. If in (i), $\{\mathcal{I}(1), \dots, \mathcal{I}(m)\}$ is a decreasing and convex sequence, or if in (ii) $\eta < 0$, then instead of simulating Z , we simulate Z^* : the expression of λ_k

would be in this case

$$\lambda_k = \gamma(0) + 2 \sum_{j=1}^m \left\{ \mathcal{R}(j) \cos \left(\frac{2\pi jk}{\tilde{m}} \right) + \mathcal{I}(j) \sin \left(\frac{2\pi jk}{\tilde{m}} \right) \right\}$$

and Proposition 4.2 can be applied if in addition (4.4) or (4.5) holds.

The following result extends Dietrich and Newsam (1997, Theorem 2) for modulated stationary covariances.

Proposition 4.5. *Assume that the covariance function γ is a modulated stationary covariance, that is, there exists $\phi \in \mathbb{R}$ and a real-valued covariance function r , such that $\gamma(\tau) = e^{2i\pi\phi\tau} r(\tau)$. Assume that $\{r(0), \dots, r(m)\}$ forms a decreasing and convex sequence, then, for any $m \geq n - 1$ and $k = 0, \dots, \tilde{m} - 1$, $\lambda_k \geq 0$.*

Remark 4.6. If the covariance function γ is the sum of p complex covariance functions, that is $\gamma(\tau) = \sum_{j=1}^p \gamma_j(\tau)$, then the circulant matrix \mathbf{C} into which $\mathbf{\Gamma}$ is embedded is also the sum of circulant matrices \mathbf{C}_j into which $\mathbf{\Gamma}_j$, the covariance matrices corresponding to γ_j , are embedded. Hence, the eigenvalues of \mathbf{C} can be written as $\lambda_k = \sum_{j=1}^p \lambda_k^{(j)}$ for $k = 0, \dots, \tilde{m} - 1$, where $\lambda_k^{(j)}$ are the eigenvalues of \mathbf{C}_j . As a consequence, if for $j = 1, \dots, p$, the covariance function γ_j satisfies the conditions of Proposition 4.1, 4.2 or 4.5, then the eigenvalues λ_k are non-negative.

5 Applications

5.1 Back to Examples

We now show that the results in Section 4 can be applied to Examples 2.1-2.2. In particular, for such classes the minimal embedding is sufficient to ensure the non-negativeness of \mathbf{C} . The method is therefore exact for these examples.

5.1.1 Modulated stationary processes

Proposition 4.1 (iii) applies to real covariances functions satisfying the assumptions in Proposition 1 of Craigmile (2003). Typical examples are the covariance functions

of a FARIMA process with fractional difference parameter $d \in [-1/2, 0)$ (see Equation (2.5)) and the covariance function of a fractional Gaussian noise with Hurst parameter $H \in (0, 1/2)$. For these two examples, Proposition 4.5 completes the result, since it can be checked that the aforementioned covariance functions are decreasing and convex when $d \in (0, 1/2]$ for the FARIMA process and when $H \in (1/2, 1)$ for the fractional Gaussian noise.

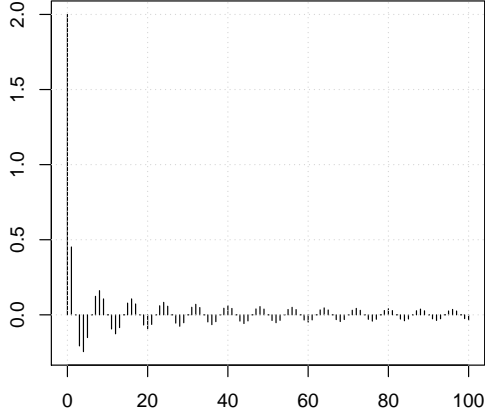
Referring to Berg and Forst (1978), here is a list of other examples with positive, decreasing and convex covariance functions, thus satisfying Proposition 4.5: (a) the mapping $\tau \mapsto r(\tau; \alpha, \beta) = \sigma^2(1 + |\tau|^\alpha)^{-\beta}$, $\alpha \in (0, 1]$, $\beta > 0$, $\sigma > 0$ and $\tau \in \mathbb{R}$; (b) $r(\tau) = \sigma^2(1 - |\tau|)_+^n$, $n > 0$ and $\sigma > 0$; (c) $r(\tau) = \sigma^2 \int_{(0, \infty)} (1 - \xi|\tau|)_+ \mu(d\xi)$, for μ any positive and bounded measure and $\sigma > 0$; (d) $r(\tau) = \sigma^2 e^{-\alpha|\tau|}$, $\alpha > 0$ and $\sigma > 0$; (e) $r(\tau) = \sigma^2 \rho^{|\tau|}$, $0 < \rho < 1$ and $\sigma > 0$.

This, in particular, covers the modulated exponential covariance (2.4) and the complex AR(1) process presented in Example 2.1. Finally, Remark 4.6 can be applied to embrace examples where the covariance is the sum of modulated FARIMA or fractional Gaussian noise covariance functions. Figure 1 illustrates this section.

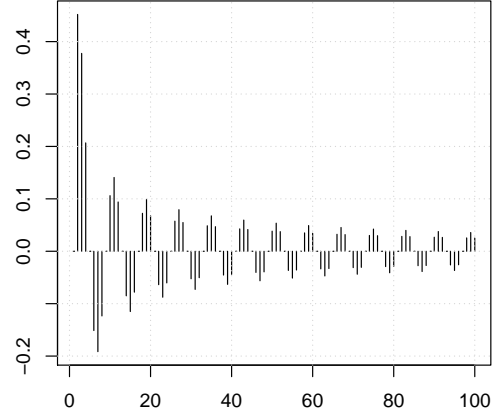
5.1.2 Circular complex fBm

The circular complex fBm has covariance given by (2.8). We omit the case $H = 1/2$, which, as outlined earlier, leads to another parametrization of the covariance function. We remind that this covariance function is positive definite under the condition that $\eta \leq |\tan(\pi H)|$. We study separately the cases $H \in (0, 1/2)$ and $H \in (1/2, 1)$. When $H \in (0, 1/2)$, Proposition 4.1 (ii) applies with the restriction $\eta < \min\{1, \tan(\pi H)\}$.

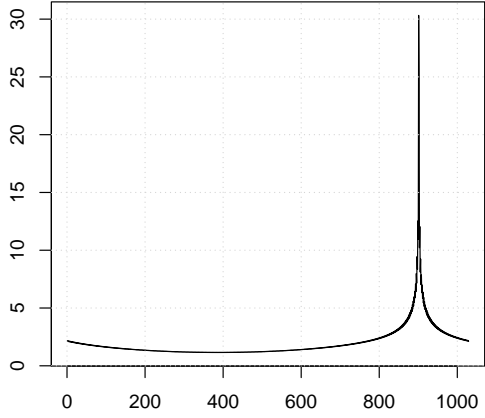
When $H \in (1/2, 1)$, we apply Proposition 4.2 (ii). In this setting, $\gamma_{\mathcal{R}}(j)$ corresponds to the covariance function of a fractional Gaussian noise with Hurst exponent H . This covariance function is decreasing and convex for any $H \in (1/2, 1)$. Let us now comment (4.5). We can establish that the sequence $\{\Delta^2 r(j)\}_{j \geq 1}$ decreases hyperbolically to 0 with a rate of convergence j^{2H-2} and since the Féjer and conjugate Féjer kernels are bounded, it can be expected that S_m is quite small. Added to the fact that $\gamma_{\mathcal{R}}(m) \rightarrow 0$, we can really expect that (4.5) is not restrictive.



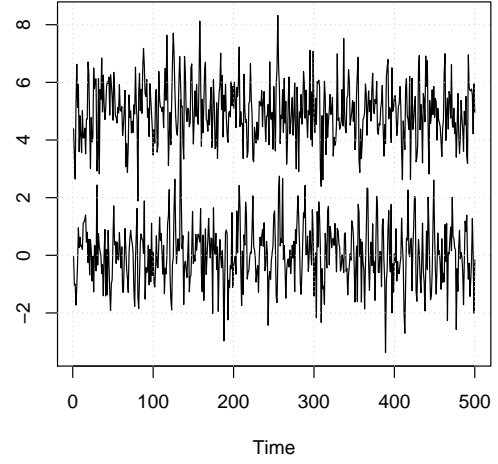
(a) Real part of the covariance function



(b) Imaginary part of the covariance function



(c) Eigenvalues of the circulant matrix \mathbf{C}



(d) Real (top) and Imaginary parts of $Z(t)$

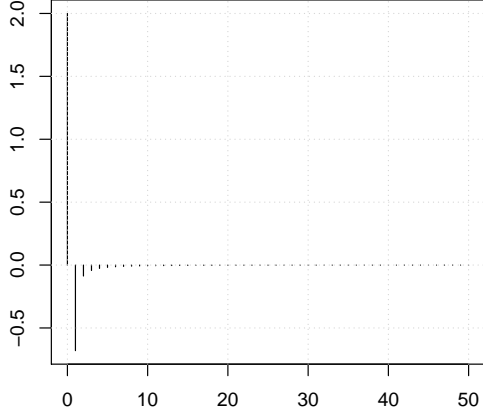
Figure 1: Simulation details for the example of a modulated FARIMA(0, d , 0) process with unit variance, fractional parameter $d = 0.2$ and phase parameter $\phi = 1/8$. The sample size is $n = 500$ and \mathbf{C} is chosen as a $m \times m$ matrix with $m = 3 \times 5 \times 7 = 514$. For (d), a constant is added to the real part of $Z(t)$ to differentiate the two sample paths.

For several values of m , we have evaluated the value of \tilde{H} such that for the maximal value of the parameter η allowed by the model, that is $\eta = |\tan(\pi H)|$, $\Delta^2 \gamma_{\mathcal{R}}(0) + S_m\{|\tan(\pi H)|\} \geq |\tan(\pi H)| \gamma_{\mathcal{R}}(m)$ is valid for any $H \in (1/2, \tilde{H})$. We obtained the values $\tilde{H} = 0.939, 0.954$ and 0.964 when $m = 100, 1000$ and 10000 . The conditions (4.4)–(4.5) could be slightly refined, for instance by noticing that $K_{m-1}(k/\tilde{m}) \geq 1$. We do not present this since, for instance regarding the value of \tilde{H} investigated above, we did not notice significant improvements.

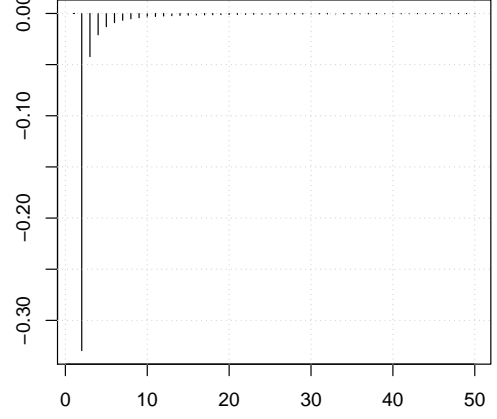
Figures 2, 3 and 4 illustrate this section. For $H = 0.2$ and $H = 0.8$. Figures 2-3 depict the sample paths of the circular complex fBm with length $n = 10^6$. Four seconds is the timing required to generate each realization. As expected, we observe that the higher H the more regular the sample path. We can check that despite the plot of the eigenvalues exhibit different shapes, the eigenvalues are all non-negative. Finally, using the R function `acf`, the circularity property is graphically tested in Figure 4. The difference between the estimates $\gamma_{\mathcal{RI}}$ and $-\gamma_{\mathcal{IR}}(j)$ are very small, which convinces us that the realization should be circular.

5.2 Confidence interval for the Hurst exponent of a circular complex fBm

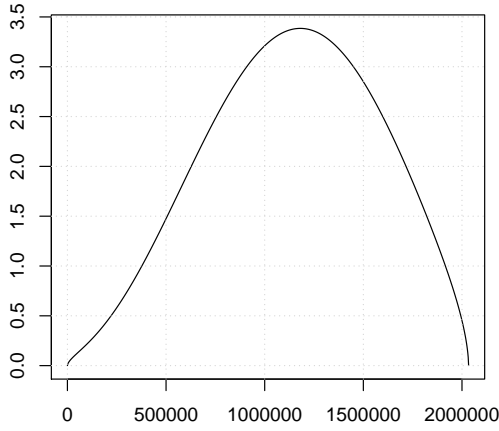
In this section, we suppose to have access to a sampled version of circular complex fBm. We extend an estimation method to estimate the Hurst exponent and illustrate how the simulation method can be used to derive confidence intervals using parametric Bootstrap samples. Many methods allow to estimate the self-similarity parameter of a fractional Brownian motion efficiently. We consider here the discrete variations method, see Kent and Wood (1997); Istaş and Lang (1997); Coeurjolly (2001). We focus only on the estimation of the Hurst exponent H to illustrate the simulation method. However, we are convinced that using the mentioned papers, estimates for the parameters η and σ^2 can be easily derived.



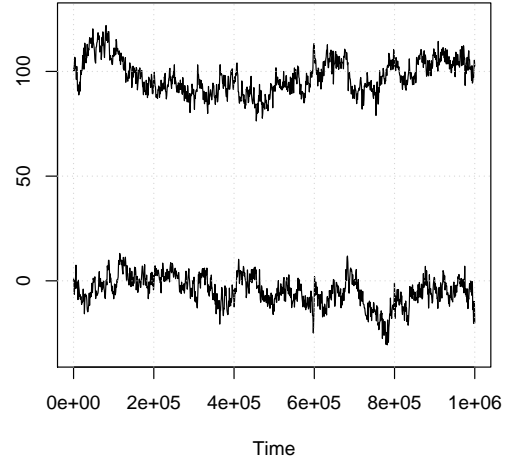
(a) Real part of the covariance function



(b) Imaginary part of the covariance function

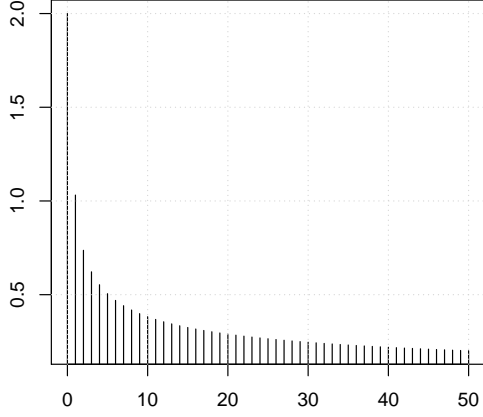


(c) Eigenvalues of the circulant matrix \mathbf{C}

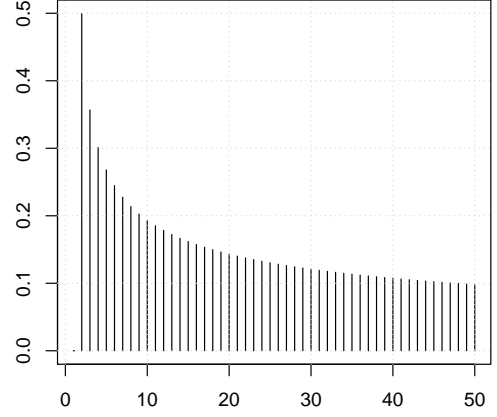


(d) Real (top) and Imaginary parts of $\tilde{Z}(t)$

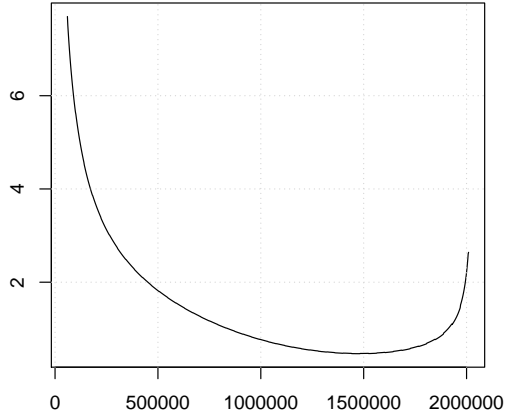
Figure 2: Simulation details for the example of a circular complex fBm with unit variance, Hurst exponent $H = 0.8$ and $\eta = \frac{2}{3}|\tan(\pi H)|$. The sample size is $n = 10^6$ and \mathbf{C} is chosen as a $m \times m$ matrix with $m = 2033647$. For (d), a constant is added to the real part of $Z(t)$ to differentiate the two sample paths.



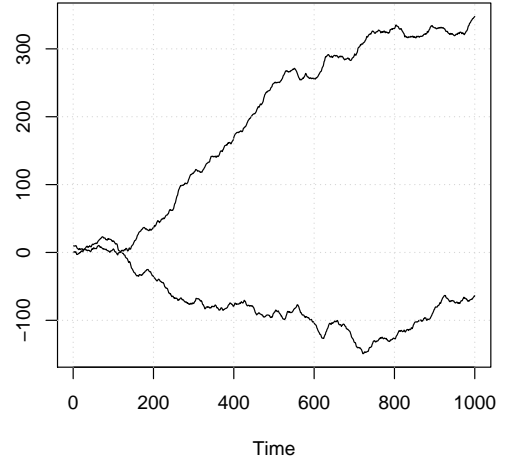
(a) Real part of the covariance function



(b) Imaginary part of the covariance function

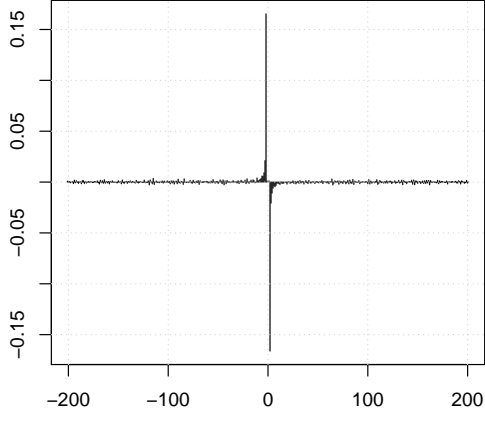


(c) Eigenvalues of the circulant matrix \mathbf{C}

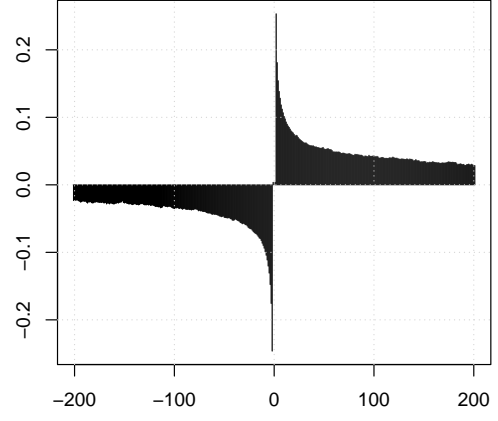


(d) Real (top) and Imaginary parts of $\tilde{Z}(t)$

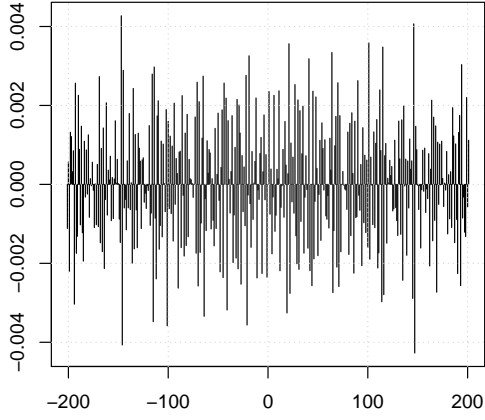
Figure 3: Simulation details for the example of a circular complex fBm with unit variance, Hurst exponent $H = 0.8$ and $\eta = \frac{2}{3}|\tan(\pi H)|$. The sample size is $n = 10^6$ and \mathbf{C} is chosen as a $m \times m$ matrix with $m = 2033647$. For (c), we focus on the eigenvalues λ_k for $k = 50000, \dots, 2 \times 10^6$. The other ones are very large. For (d), a constant is added to the real part of $Z(t)$ to differentiate the two sample paths.



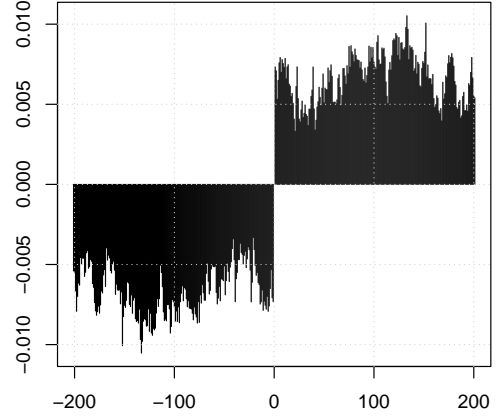
(a) $H = 0.2, \hat{\gamma}_{\mathcal{RI}}(j)$



(b) $H = 0.8, \hat{\gamma}_{\mathcal{RI}}(j)$



(c) $H = 0.2, \hat{\gamma}_{\mathcal{RI}}(j) - \{-\hat{\gamma}_{\mathcal{IR}}(j)\}$



(d) $H = 0.8, \hat{\gamma}_{\mathcal{RI}}(j) - \{-\hat{\gamma}_{\mathcal{IR}}(j)\}$

Figure 4: Verification of the circularity property. The computation of empirical cross-covariances are based on a discrete sample path of length $n = 10^6$ of a circular complex fBm with variance 1 and $\eta = \frac{2}{3} |\tan(\pi H)|$.

Let ℓ and q be two positive integers. We consider the following set of filters $\mathcal{A}_{\ell,q}$:

$$\mathcal{A}_{\ell,q} = \left\{ (a_k)_{k \in \mathbb{Z}} : a_k = 0, \forall k \in \mathbb{Z}^- \setminus \{0\} \cup \{\ell + 1, \dots, \infty\} \right. \\ \left. \text{and } \sum_{k \in \mathbb{Z}} k^l a_k = 0, \forall l = 0, \dots, q-1, \sum_{k \in \mathbb{Z}} k^q a_k \neq 0 \right\}.$$

Typical examples are the difference filter $\delta_{l,0} - \delta_{l,1}$ and its compositions, Daubechies wavelet filters, and any known wavelet filter with compact support and a sufficient number of vanishing moments. For $a \in \mathcal{A}_{\ell,q}$ and an integer $\mu \geq 1$ we define the μ th dilated version of a , say a^μ as

$$a_k^\mu = \begin{cases} a_{k/\mu} & \text{if } k \in \mu\mathbb{Z} \\ 0 & \text{if } k \notin \mu\mathbb{Z}. \end{cases}$$

Apparently, $a^1 = a$ and $a^\mu \in \mathcal{A}_{\ell,q}$ for any μ . The μ th dilated version is thus simply obtained by oversampling a by a factor of μ , *i.e.* by adding $\mu - 1$ zeros between each of the first $\ell + 1$ coefficients of the impulse response a_k . We denote by \tilde{Z}^μ a discretized sample path of a circular complex fBm \tilde{Z} at times $t = 0, \dots, n-1$ filtered with a^μ . In other words

$$\tilde{Z}^\mu(j) = \sum_{k=0}^{\ell} a_k^\mu \tilde{Z}(j-k), \quad j = \ell, \dots, n-1.$$

Let $\mu, \mu' \geq 1$, we denote by $\gamma_{Z^\mu, Z^{\mu'}}(\tau)$ the cross-covariance function between \tilde{Z}^μ and $\tilde{Z}^{\mu'}$.

By definition of a , we have

$$\gamma_{Z^\mu, Z^{\mu'}}(\tau) = \sum_{q=0}^{\mu\ell} \sum_{r=0}^{\mu'\ell} a_q^\mu a_r^{\mu'} \mathbb{E} \left\{ \tilde{Z}(\tau + k - q) \tilde{Z}(k - r) \right\} \\ = -\sigma^2 \sum_{q,r=0}^{\ell} \{1 - \mathbf{i}\eta \operatorname{sign}(\tau + \mu'r - \mu q)\} |\tau + \mu'r - \mu q|^{2H}.$$

In particular, we can check that

$$\operatorname{Var}\{\tilde{Z}^\mu(j)\} = \gamma_{Z^\mu, Z^\mu}(0) = \mu^{2H} \left(-\sigma^2 \sum_{q,r=0}^{\ell} a_q a_r |q - r|^{2H} \right).$$

Now, let $S^2(\mu)$ be the empirical mean squared modulus at scale μ given by

$$S^2(\mu) = \frac{1}{n - \mu\ell} \sum_{j=\mu\ell}^{n-1} |\tilde{Z}^\mu(j)|^2.$$

Since $S^2(\mu)$ is expected to be close to $\kappa\mu^{2H}$ where κ is independent of H , we propose to estimate H by a linear regression of $\log S^2(\mu)$ on $\log \mu$ for $\mu \in \mathcal{M} \subset \mathbb{N}^M \setminus \{0\}$, a collection of dilation factors. This estimate is given by

$$\hat{H} = \frac{\mathbf{L}^\top}{2\mathbf{L}^\top \mathbf{L}} \{\log S^2(\mu)\}_{\mu \in \mathcal{M}} \quad \text{with} \quad \mathbf{L} = \left(\log \mu - M^{-1} \sum_{\mu} \log \mu \right)_{\mu \in \mathcal{M}}.$$

Such an estimate is very close to the ones proposed by Coeurjolly (2001) and Amblard and Coeurjolly (2011) to estimate the Hurst exponent of a fBm and the Hurst exponents of a multivariate fBm respectively. We simply exploit the complex characteristic of the process. Using theoretical results from the previous papers, we have the following asymptotic result, given without proof.

Proposition 5.1. *As $n \rightarrow \infty$, \hat{H} tends to H with probability 1, and if $p > H + 1/4$*

$$\sqrt{n}(\hat{H} - H) \rightarrow N \left\{ 0, \frac{\mathbf{L}^\top \Sigma_M \mathbf{L}}{2(\mathbf{L}^\top \mathbf{L})^2} \right\}, \quad (5.1)$$

in distribution, where Σ_M is the $M \times M$ matrix with entries

$$(\Sigma_M)_{\mu\mu'} = \sum_{k \in \mathbb{Z}} \frac{|\gamma_{Z^\mu, Z^{\mu'}}(k)|^2}{\gamma_{Z^\mu, Z^\mu}(0)\gamma_{Z^{\mu'}, Z^{\mu'}}(0)}, \quad \mu, \mu' \in \mathcal{M}. \quad (5.2)$$

The condition $p > H + 1/4$ is quite standard for such problems and expresses the fact that a circular complex fBm needs to be filtered with a filter with at least two zeroes moments to ensure a Gaussian behaviour for any $H \in (0, 1)$. In the rest of this section, we intend to compare several approaches for constructing confidence intervals for H . We assume that both parameters σ^2 and η are known. The first approach, referred to as CLT, uses (5.1) to construct asymptotic confidence intervals. The series involved in (5.2) are truncated. The two other ones are based on parametric Bootstrap. We considered the percentile Bootstrap and Studentized Bootstrap methods, referred to as PPB and SPB respectively, to propose confidence intervals. Given a sample path of a circular complex fBm, we use 2000 replications of the fitted model for these parametric Bootstrap methods. Table 2 reports the empirical coverage rate and the mean length of 95% confidence intervals based on 2000 replications of a circular complex fBm for different values of n, η, H . The variance σ^2 is set to 1. In terms of coverage rate, the confidence intervals tend to be very

comparable. The PBP method produces confidence intervals with length larger than the two other methods. Amongst the CLT and the SPB approaches, the latter seems to be slightly better in terms of confidence intervals. It is worth noticing that even for small sample sizes, the CLT method is very competitive.

	$H = 0.2$			$H = 0.8$		
	CLT	PPB	SPB	CLT	PPB	SPB
$n = 100$						
$\frac{1}{3}\eta_{\max}$	94 (22.0)	95 (22.8)	95 (21.9)	94 (27.9)	96 (30.1)	96 (27.9)
$\frac{2}{3}\eta_{\max}$	94 (23.7)	96 (24.4)	96 (23.6)	94 (31.2)	94 (33.3)	94 (31.1)
$n = 500$						
$\frac{1}{3}\eta_{\max}$	95 (9.8)	95 (9.9)	95 (9.8)	95 (12.5)	96 (12.8)	96 (12.5)
$\frac{2}{3}\eta_{\max}$	95 (10.6)	95 (10.7)	95 (10.6)	94 (13.9)	92 (14.4)	92 (13.9)
$n = 1000$						
$\frac{1}{3}\eta_{\max}$	96 (7.0)	96 (7.0)	96 (6.9)	94 (8.8)	95 (9.0)	95 (8.8)
$\frac{2}{3}\eta_{\max}$	95 (7.5)	95 (7.5)	95 (7.5)	95 (9.9)	94 (10.1)	94 (9.8)

Table 2: Empirical coverage rate and mean length, between brackets, of 95% confidence intervals built using (5.1) (method CLT) or Bootstrap techniques (methods PPB and SPB). The simulation is based on 2000 replications of circular complex fBm for different sample sizes and different values of H and η . Empirical coverage rates are reported in percentage and mean lengths are multiplied by 100.

A Proofs

A.1 Auxiliary lemmas

The following definitions and results are quite standard in Fourier theory. We refer the reader to Zygmund (2002).

Lemma A.1. *Let $p \in \mathbb{N} \setminus \{0\}$. The Dirichlet and Féjer kernels are respectively defined by*

$$D_p(\omega) = 1 + 2 \sum_{j=1}^p \cos(2\pi j\omega) = \begin{cases} \frac{\sin\{\pi\omega(2p+1)\}}{\sin(\pi\omega)} & \text{if } \omega \in \mathbb{R} \setminus \mathbb{Z} \\ 2p+1 & \text{if } \omega \in \mathbb{Z}, \end{cases}$$

$$K_p(\omega) = \sum_{j=0}^p D_j(\omega) = \begin{cases} \left[\frac{\sin\{\pi\omega(p+1)\}}{\sin(\pi\omega)} \right]^2 \geq 0, & \text{if } \omega \in \mathbb{R} \setminus \mathbb{Z} \\ (p+1)(2p+1) & \text{if } \omega \in \mathbb{Z}. \end{cases}$$

The conjugate Dirichlet and Féjer kernels are respectively defined by

$$\tilde{D}_p(\omega) = 2 \sum_{j=0}^p \sin(2\pi j\omega) = \begin{cases} \frac{\cos(\pi\omega)}{\sin(\pi\omega)} - \frac{\cos\{\pi\omega(2p+1)\}}{\sin(\pi\omega)} & \text{if } \omega \in \mathbb{R} \setminus \mathbb{Z} \\ 0 & \text{if } \omega \in \mathbb{Z}, \end{cases}$$

$$\tilde{K}_p(\omega) = \sum_{j=0}^p \tilde{D}_j(\omega) = \begin{cases} \frac{(p+1)\sin(2\pi\omega) - \sin\{2\pi\omega(p+1)\}}{2\sin(\pi\omega)^2} & \text{if } \omega \in \mathbb{R} \setminus \mathbb{Z}, \\ 0 & \text{if } \omega \in \mathbb{Z}. \end{cases}$$

Moreover, the conjugate Féjer kernel satisfies $\tilde{K}_p(\omega) \geq 0$ whenever $\omega \in [k, k + 1/2]$, for any $k \in \mathbb{Z}$.

Proof. Except for the last result, the proofs can be found in Zygmund (2002). For the last assertion, we need to prove that $p \sin(t) - \sin(pt)$ is non-negative for $t \in [0, \pi]$ which is proved as follows

$$\begin{aligned} \sin(pt) &\leq |\sin(pt)| = |\sin\{(p-1)t\} \cos(t) + \cos\{(p-1)t\} \sin(t)| \\ &\leq |\sin\{(p-1)t\}| + |\sin(t)| \leq \dots \leq p|\sin(t)| = p \sin(t) \end{aligned}$$

when $t \in [0, \pi]$. □

The following result is a summation by parts formula mainly used in the proof of Proposition 4.2.

Lemma A.2. *Let $n \geq 1$ and $(f_0, \dots, f_n)^\top$ and $(g_0, \dots, g_n)^\top$ be two vectors of real numbers then,*

$$\sum_{j=0}^n f_j g_j = f_n \sum_{j=0}^n g_j + \sum_{j=0}^{n-1} (f_j - f_{j+1}) \sum_{\ell=0}^j g_\ell. \quad (\text{A.1})$$

A.2 Proof of Proposition 3.1

Proof. For $k = 0, \dots, \tilde{m} - 1$, since $(\tilde{m}^{1/2} \Lambda^{1/2} \mathbf{Q}^* \mathbf{N}_{\tilde{m}})_k$ is a complex normal random variable, we identify it to $\sqrt{\lambda_k}(S'_k + i T'_k)/\tilde{m}$ where S'_k and T'_k are the Gaussian random variables given by

$$S'_k = \sum_{j=0}^{\tilde{m}-1} \cos\left(\frac{2\pi j k}{\tilde{m}}\right) (\mathbf{N}_{\tilde{m}})_j \quad \text{and} \quad T'_k = \sum_{j=0}^{\tilde{m}-1} \sin\left(\frac{2\pi j k}{\tilde{m}}\right) (\mathbf{N}_{\tilde{m}})_j.$$

The proof reduces to calculate $\text{Cov}(U_k, U_{k'})$ for $k, k' = 0, \dots, \tilde{m} - 1$ and $U_k = S'_k$ or T'_k .

Let $k, k' \in \{0, \dots, \tilde{m} - 1\}$. First, by Lemma A.1, it can be checked that

$$\begin{aligned} \text{Cov}(S'_k, S'_{k'}) &= \sum_{j=0}^{\tilde{m}-1} \cos\left(\frac{2\pi j k}{\tilde{m}}\right) \cos\left(\frac{2\pi j k'}{\tilde{m}}\right) \\ &= \frac{1}{2} \left[\sum_{j=0}^{\tilde{m}-1} \cos\left\{\frac{2\pi j(k-k')}{\tilde{m}}\right\} + \sum_{j=0}^{\tilde{m}-1} \cos\left\{\frac{2\pi j(k+k')}{\tilde{m}}\right\} \right] \\ &= \frac{1}{2} + \frac{1}{4} D_{\tilde{m}-1}\left(\frac{k-k'}{\tilde{m}}\right) + \frac{1}{4} D_{\tilde{m}-1}\left(\frac{k+k'}{\tilde{m}}\right) \\ &= \begin{cases} \frac{1}{2} + \frac{1}{4} \{2(\tilde{m}-1)\} = \frac{\tilde{m}}{2} & \text{if } k = k' \\ \frac{1}{2} + \frac{1}{4} \{2(\tilde{m}-1)\} = \frac{\tilde{m}}{2} & \text{if } k + k' = \tilde{m} \\ \frac{1}{2} + \frac{1}{4} \frac{\sin\{\pi(k-k')(2\tilde{m}-1)/\tilde{m}\}}{\sin\{\pi(k-k')/\tilde{m}\}} + \frac{1}{4} \frac{\sin\{\pi(k+k')(2\tilde{m}-1)/\tilde{m}\}}{\sin\{\pi(k+k')/\tilde{m}\}} = 0 & \text{otherwise.} \end{cases} \end{aligned}$$

We remark that $k + k' = \tilde{m}$ takes place only when $k \wedge k' > 0$. Second, with the same ideas

$$\begin{aligned} \text{Cov}(T'_k, T'_{k'}) &= \sum_{j=0}^{\tilde{m}-1} \sin\left(\frac{2\pi j k}{\tilde{m}}\right) \sin\left(\frac{2\pi j k'}{\tilde{m}}\right) \\ &= \frac{1}{2} \left[\sum_{j=0}^{\tilde{m}-1} \cos\left\{\frac{2\pi j(k-k')}{\tilde{m}}\right\} - \sum_{j=0}^{\tilde{m}-1} \cos\left\{\frac{2\pi j(k+k')}{\tilde{m}}\right\} \right] \\ &= \frac{1}{4} D_{\tilde{m}-1}\left(\frac{k-k'}{\tilde{m}}\right) - \frac{1}{4} D_{\tilde{m}-1}\left(\frac{k+k'}{\tilde{m}}\right) \\ &= \begin{cases} \frac{\tilde{m}}{2} & \text{if } k = k' \\ -\frac{\tilde{m}}{2} & \text{if } k + k' = \tilde{m} \\ 0 & \text{otherwise.} \end{cases} \end{aligned}$$

Third,

$$\begin{aligned}
\text{Cov}(S'_k, T'_{k'}) &= \sum_{j=0}^{\tilde{m}-1} \cos\left(\frac{2\pi j k}{\tilde{m}}\right) \sin\left(\frac{2\pi j k'}{\tilde{m}}\right) \\
&= \frac{1}{2} \left[\sum_{j=0}^{\tilde{m}-1} \sin\left\{\frac{2\pi j(k+k')}{\tilde{m}}\right\} - \sum_{j=0}^{\tilde{m}-1} \sin\left\{\frac{2\pi j(k-k')}{\tilde{m}}\right\} \right] \\
&= \frac{1}{4} \tilde{D}_{\tilde{m}-1}\left(\frac{k+k'}{\tilde{m}}\right) - \frac{1}{4} \tilde{D}_{\tilde{m}-1}\left(\frac{k-k'}{\tilde{m}}\right) \\
&= 0,
\end{aligned}$$

whereby we deduce the result. \square

A.3 Proof of Proposition 3.2

Proof. It is clear that $\mathbf{H} = \mathbf{Q}\Lambda^{1/2}(\mathbf{Q}^*)^2\Lambda^{1/2}\mathbf{Q}$. Using, the proof of Proposition 3.1, we can check that for $j, k = 0, \dots, \tilde{m}-1$

$$\begin{aligned}
(\mathbf{Q}^*)_{jk}^2 &= \tilde{m}^{-1} \sum_{\ell=0}^{\tilde{m}-1} \left\{ \cos\left(\frac{2\pi j \ell}{\tilde{m}}\right) \cos\left(\frac{2\pi k \ell}{\tilde{m}}\right) - \sin\left(\frac{2\pi j \ell}{\tilde{m}}\right) \sin\left(\frac{2\pi k \ell}{\tilde{m}}\right) \right\} \\
&\quad + \mathbf{i} \tilde{m}^{-1} \sum_{\ell=0}^{\tilde{m}-1} \left\{ \sin\left(\frac{2\pi j \ell}{\tilde{m}}\right) \cos\left(\frac{2\pi k \ell}{\tilde{m}}\right) + \cos\left(\frac{2\pi j \ell}{\tilde{m}}\right) \sin\left(\frac{2\pi k \ell}{\tilde{m}}\right) \right\} \\
&= \begin{cases} 1 & \text{if } j+k = \tilde{m} \\ 0 & \text{otherwise.} \end{cases}
\end{aligned}$$

Let \mathbf{L} be the $\tilde{m} \times \tilde{m}$ matrix given by $(\mathbf{L})_{jk} = \sqrt{\lambda_j \lambda_{\tilde{m}-j}}$, if $j \wedge k > 0$ and $j+k = \tilde{m}$ and 0 otherwise. We have, $\Lambda^{1/2}(\mathbf{Q}^*)^2\Lambda^{1/2} = \mathbf{L}$. The result follows from

$$(\mathbf{QL})_{jk} = \tilde{m}^{-1/2} \sum_{\ell=0}^{\tilde{m}-1} e^{-\frac{2\mathbf{i}\pi j \ell}{\tilde{m}}} (L)_{\ell k} = \tilde{m}^{-1/2} e^{-\frac{2\mathbf{i}\pi j(\tilde{m}-k)}{\tilde{m}}} \sqrt{\lambda_k \lambda_{\tilde{m}-k}} \mathbf{1}(k > 0) = (\mathbf{Q}^*\mathbf{V})_{jk},$$

where $\mathbf{V} = \text{diag}(v_k, k = 0, \dots, \tilde{m}-1)$ is the diagonal matrix with elements given by $v_0 = 0$ and $v_k = \sqrt{\lambda_k \lambda_{\tilde{m}-k}}$ for $k \geq 1$. \square

A.4 Proof of Proposition 3.3

Proof. We proceed similarly to the proof of Proposition 3.1. We identify the Gaussian random variable W_k to $\sqrt{\lambda_k/2}(S'_k + \mathbf{i}T'_k)/\tilde{m}$ where S'_k and T'_k are the Gaussian random

variables given by

$$\begin{aligned} S'_k &= \sum_{j=0}^{\tilde{m}-1} \left\{ \cos\left(\frac{2\pi jk}{\tilde{m}}\right) (\mathbf{N}_{\tilde{m}})_{1,j} - \sin\left(\frac{2\pi jk}{\tilde{m}}\right) (\mathbf{N}_{\tilde{m}})_{2,j} \right\} \\ T'_k &= \sum_{j=0}^{\tilde{m}-1} \left\{ \sin\left(\frac{2\pi jk}{\tilde{m}}\right) (\mathbf{N}_{\tilde{m}})_{1,j} + \cos\left(\frac{2\pi jk}{\tilde{m}}\right) (\mathbf{N}_{\tilde{m}})_{2,j} \right\}. \end{aligned}$$

We leave the reader to check that for any $k, k' \in \{0, \dots, \tilde{m} - 1\}$, $\text{Cov}(S'_k, S'_{k'}) = \text{Cov}(T'_k, T'_{k'}) = \tilde{m}\delta_{kk'}$ and $\text{Cov}(S'_k, T'_{k'}) = 0$, whereby we deduce the result. \square

A.5 Proof of Proposition 3.4

Proof. For each $x > 0$,

$$\begin{aligned} \mathbb{P}\left(\max_{j=0, \dots, n-1} \sigma_j^{-1} |\Delta_j| > x\right) &= 1 - \mathbb{P}\left(\bigcap_{j=0}^{n-1} \{\sigma_j^{-1} |\Delta_j| \leq x\}\right) \\ &\leq 1 - \mathbb{P}\left[\bigcap_{j=0}^{n-1} \left\{|\text{Re}(\Delta_j)| \leq \frac{x\sigma_j}{\sqrt{2}}, |\text{Im}(\Delta_j)| \leq \frac{x\sigma_j}{\sqrt{2}}\right\}\right]. \end{aligned}$$

From Dunn (1958, 1959)

$$\mathbb{P}\left(\max_{j=0, \dots, n-1} \sigma_j^{-1} |\Delta_j| > x\right) \leq 1 - \prod_{j=0}^{n-1} \mathbb{P}\left\{|\text{Re}(\Delta_j)| \leq \frac{x\sigma_j}{\sqrt{2}}\right\} \mathbb{P}\left\{|\text{Im}(\Delta_j)| \leq \frac{x\sigma_j}{\sqrt{2}}\right\}$$

whereby we deduce the result. \square

A.6 Proof of Proposition 4.1

Proof. (i) For any $k = 0, \dots, \tilde{m} - 1$, we have

$$\lambda_k \geq \gamma(0) + 2 \sum_{j=1}^m \{\mathcal{R}(j) - s\mathcal{I}(j)\} = \sum_{|j| \leq m} \{\mathcal{R}(j) - s \text{sign}(j)\mathcal{I}(j)\} =: A_m.$$

Since $A_{m+1} - A_m = 2\mathcal{R}(m+1) - s\{\mathcal{I}(m+1) - \mathcal{I}(-m-1)\} \leq 0$, $\{A_m\}_{m \geq 1}$ is a decreasing sequence. By Assumption, $\mathbf{S}(\omega) = \sum_{j \in \mathbb{Z}} \mathbf{M}(j) e^{-2i\pi j\omega}$ is a Hermitian non-negative definite matrix for every ω . In particular, for $y = (1, -s)^\top$ and $\omega = 0$, we have

$$y^\top \mathbf{S}(0) y = \sum_{j \in \mathbb{Z}} \{\mathcal{R}(j) - s\mathcal{I}(j)\} \geq 0,$$

whereby we deduce that $\lambda_k \geq \lim_{m \rightarrow \infty} y^\top \mathbf{S}(0)y \geq 0$.

(ii) In this setting, $\mathcal{R}(j) = 2\gamma_{\mathcal{R}}(j)$ and $\mathcal{I}(j) = 2\gamma_{\mathcal{RI}}(j) = 2\eta \text{sign}(j)\gamma_{\mathcal{R}}(j)$. Hence, the matrix $\mathbf{M}(j)$ given by (4.2) takes the form

$$\mathbf{M}(j) = \gamma_{\mathcal{R}}(j) \begin{pmatrix} 1 & \eta \\ \eta & 1 \end{pmatrix}.$$

This indeed corresponds to the covariance matrix of a stationary bivariate process, say \tilde{Z} . By the same argument than Craigmile (2003)[Proposition 1] in the real case, if $\gamma_{\mathcal{R}}$ is not summable then the spectrum at zero frequency is negative infinity, an impossibility. Hence, \tilde{Z} admits a well-defined spectral density matrix and Proposition 4.1 applies.

(iii) Let $\tilde{\phi} = \phi\tilde{m}$. Using standard trigonometric identities, the expression of λ_k reduces to

$$\lambda_k = r(0) + 2 \sum_{j=1}^m r(j) \cos \left\{ \frac{2\pi j}{\tilde{m}} (k + \tilde{\phi}) \right\}. \quad (\text{A.2})$$

The rest of the proof follows the same lines as for the proof of (i). \square

A.7 Proof of Proposition 4.2

Proof. Lemmas A.1–A.2 are used in this proof. By the summation by parts formula, we have

$$\begin{aligned} 2 \sum_{j=0}^{\tilde{m}-1} \mathcal{R}(j) \cos \left(\frac{2\pi j k}{\tilde{m}} \right) &= \mathcal{R}(m) \left\{ D_m \left(\frac{k}{\tilde{m}} \right) + 1 \right\} + \sum_{j=0}^{\tilde{m}-1} \Delta \mathcal{R}(j) \left\{ D_j \left(\frac{k}{\tilde{m}} \right) + 1 \right\} \\ 2 \sum_{j=1}^{\tilde{m}-1} \mathcal{I}(j) \sin \left(\frac{2\pi j k}{\tilde{m}} \right) &= \mathcal{I}(m) \tilde{D}_m \left(\frac{k}{\tilde{m}} \right) + \sum_{j=1}^{\tilde{m}-1} \Delta \mathcal{I}(j) \tilde{D}_j \left(\frac{k}{\tilde{m}} \right). \end{aligned}$$

Reinjecting these equations in (4.1) leads to

$$\lambda_k = -\mathcal{I}(m) \tilde{D}_m \left(\frac{k}{\tilde{m}} \right) + \sum_{j=1}^{m-1} (-\Delta \mathcal{I})(j) \tilde{D}_j \left(\frac{k}{\tilde{m}} \right) + \sum_{j=0}^{m-1} \Delta \mathcal{R}(j) D_j \left(\frac{k}{\tilde{m}} \right).$$

Another application of Lemma A.2 allows us to obtain (4.3).

(i) This assertion ensues from Lemma A.1 and condition (4.4).

(ii) This point is a particular case of (i). \square

A.8 Proof of Proposition 4.5

Proof. Starting from (A.2), if we apply twice a summation by parts formula, we obtain

$$\lambda_k = \Delta r(m-1)K_{m-1}\left(\frac{k+\tilde{\phi}}{\tilde{m}}\right) + \sum_{j=0}^{m-2}(\Delta^2 r)(j)K_j\left(\frac{k+\tilde{\phi}}{\tilde{m}}\right), \quad (\text{A.3})$$

which is non-negative by assumption and Lemma A.1. \square

References

- Amblard, P.-O. & Coeurjolly, J.-F. (2011). Identification of the multivariate fractional Brownian motion. *IEEE Transactions on Signal Processing* **59**(11), 5152–5168.
- Amblard, P.-O., Gaeta, M. & Lacoume, J.-L. (1996). Statistics for complex variables and signals — Part II: signals. *Signal Processing* **53**(1), 15–25.
- Amblard, P.-O., Coeurjolly, J.-F., Lavancier, F. & Philippe, A. (2013). Basic properties of the multivariate fractional Brownian motion. In: *Séminaires et Congrès, Self-similar processes and their applications*, volume 28, 65–87.
- Berg, C. & Forst, G. (1978). *Potential theory on locally compact Abelian groups*, volume 87. Springer Science & Business Media.
- Brockwell, P. & Davis, R. (1987). *Time Series: Theory and Methods*. Springer Verlag, New York.
- Chan, G. & Wood, A. (1999). Simulation of stationary Gaussian vector fields. *Statistics and Computing* **9**(4), 265–268.
- Coeurjolly, J.-F. (2000). Simulation and identification of the fractional Brownian motion: a bibliographical and comparative study. *Journal of Statistical Software* **5**(7), 1–53.

- Coeurjolly, J.-F. (2001). Estimating the parameters of a fractional Brownian motion by discrete variations of its sample paths. *Statistical Inference for Stochastic Processes* **4**(2), 199–227.
- Coeurjolly, J.-F., Amblard, P.-O. & Achard, S. (2013). Wavelet analysis of the multivariate fractional Brownian motion. *ESAIM: Probability and Statistics* **17**, 592–604.
- Craigmire, P. (2003). Simulating a class of stationary Gaussian processes using the Davies–Harte algorithm, with application to long-memory processes. *Journal of Time Series Analysis* **24**(5), 505–511.
- Curtis, T. (1985). Digital signal processing for sonar. In: *Adaptive Methods in Underwater Acoustics*, Springer, 583–605.
- Davies, R. & Harte, D. (1987). Tests for Hurst effect. *Biometrika* **74**(1), 95–101.
- Davies, T. & Bryant, D. (2013). On circulant embedding for Gaussian random fields in \mathbb{R} . *Journal of Statistical Software* **55**(9), 1–21.
- Didier, G. & Pipiras, V. (2011). Integral representations of operator fractional Brownian motions. *Bernoulli* **17**(1), 1–33.
- Dietrich, C. & Newsam, G. (1997). Fast and exact simulation of stationary Gaussian processes through circulant embedding of the covariance matrix. *SIAM Journal of Scientific Computing* **18**(4), 1088–1107.
- Dunmire, B., Beach, K., Labs, K., Plett, M. & Strandness, D. (2000). Cross-beam vector doppler ultrasound for angle-independent velocity measurements. *Ultrasound in medicine & biology* **26**(8), 1213–1235.
- Dunn, O. (1958). Estimation of the means of dependent variables. *The Annals of Mathematical Statistics* **29**(4), 1095–1111.
- Dunn, O. (1959). Confidence intervals for the means of dependent, normally distributed variables. *Journal of the American Statistical Association* **54**(287), 613–621.

- Gneiting, T., Ševčíková, H., Percival, D., Schlather, M. & Jiang, Y. (2012). Fast and exact simulation of large Gaussian lattice systems in \mathbb{R}^2 : exploring the limits. *Journal of Computational and Graphical Statistics* **15**(3), 483–501.
- Helgason, H., Pipiras, V. & Abry, P. (2011). Fast and exact synthesis of stationary multivariate Gaussian time series using circulant embedding. *Signal Processing* **91**, 1123–1133.
- Helgason, H., Pipiras, V. & Abry, P. (2014). Smoothing windows for the synthesis of Gaussian stationary random fields using circulant matrix embedding. *Journal of Computational and Graphical Statistics* **23**(3), 616–635.
- Istas, J. & Lang, G. (1997). Quadratic variations and estimation of the local hölder index of a Gaussian process. In: *Annales de l’Institut Henri Poincaré*, volume 33, 407–436.
- Kent, J. & Wood, A. (1997). Estimating the fractal dimension of a locally self-similar Gaussian process by using increments. *Journal of the Royal Statistical Society. Series B (Methodological)* **55**(3), 679–699.
- Lee, E. & Messerschmitt, D. (1994). *Digital communication*. Kluwer Academic Publishers, Dordrecht, The Netherlands.
- Numerical Algorithms Group (1993). *NAG Fortran Library Manual, Mark 16: F03-F06*, volume 6. Oxford, U.K.
- Percival, D. (2006). Exact simulation of complex-valued Gaussian stationary processes via circulant embedding. *Signal Processing* **86**, 1470–1476.
- Stein, M. (2002). Fast and exact simulation of fractional Brownian surfaces. *Journal of Computational and Graphical Statistics* **11**(3), 587–599.
- Tobar, F. & Turner, R. (2015). Modelling of complex signals using Gaussian processes. In: *Acoustics, Speech and Signal Processing (ICASSP), 2015 IEEE International Conference on*, IEEE, 2209–2213.

- Tong, Y. (1982). *Probability Inequalities in Multivariate Distributions*. New York: Academic Press.
- Wood, A. & Chan, G. (1994). Simulation of stationary Gaussian processes in $[0, 1]^d$. *Journal of Computational and Graphical Statistics* **3**(4), 409–432.
- Zygmund, A. (2002). *Trigonometric Series (Third Edition, Volumes I and II combined)*. Cambridge University Press.